Proceedings of the 12th International Conference on Quasicrystals (ICQ12)

Curie Temperature and Density of States at the Fermi Level for Al–Cu–Fe Phases: β-Solid State Solution–Approximants–Icosahedral Quasicrystals

E.V. Shalaeva[a,b], A.F. Prekul[c], N.I. Shchegolikhina[c] and N.I. Medvedeva[a]

[a]Institute of Solid State Chemistry, Ural Branch RAS, Ekaterinburg, Russia

[b]Ural Federal University, Ekaterinburg, Russia

[c]Institute of Metal Physics, Ural Branch RAS, Ekaterinburg, Russia

A consistent reduction in the absolute value of the negative paramagnetic Curie temperature was found in a series of Al–Cu–Fe phases: β(CsCl)-solid state solution, noncanonical approximant (η-AlCu(Fe) phase), rational approximants (P1+P2-pentagonal phases) and icosahedral quasicrystal. For these Al–Cu–Fe phases, the decrease in the Curie temperature correlates with a reduction of the density of states at the Fermi level which was estimated from the low-temperature heat capacity measurements and first-principles calculations. The observed correlation was related to the antiferromagnetic indirect exchange interaction (Ruderman–Kittel–Kasuya–Yosida interaction) between the localized magnetic moments on Fe induced by the intrinsic structural defects in the Al–Cu–Fe phases. The weakening of Fe $3d$–Al s,p hybridization owing to the intrinsic structural defects such as vacancies, antisite defects and distortions of coordination polyhedrons is suggested to be the main mechanism of appearance of localized magnetic moments on Fe atoms.

DOI: 10.12693/APhysPolA.126.572

PACS: 75.20.–g, 71.23.Ft, 71.20.–b, 61.66.Dk

1. Introduction

Since the discovery of 3D-aperiodic quasicrystals and crystalline approximants in the Al–Cu–Fe system [1–5], much attention has been devoted to the investigation of their physical properties [6–11]. Structurally perfect icosahedral (ι) quasicrystal and its canonical approximants have been found to exhibit peculiar physical properties such as high electrical resistivity [6, 7], diamagnetism [8, 9] and a pseudogap at the Fermi level [10, 11]. These specific physical properties are considered to be due to a complex cluster local structure with Al s,p–Tm $3d$ covalent binding [7, 12, 13]. The β(CsCl)–Al(Cu,Fe) solid solution and non-canonical approximants of the Al–Cu–Fe icosahedral phase such as β-based ordered phases, for which the complex cluster local structure features are not pronounced, show neither anomalous properties nor a pseudogap effect [14–16]. At the same time, it is of special interest to investigate the physical properties, whose behavior is directly affected by structural defects, and to understand how these properties vary in the series of Al–Cu–Fe phases from β-solid solution to icosahedral phase. This is important for elucidation of electron and magnetic properties of defects and for characterization of chemical binding for these defects in quasicrystal-forming systems.

At first, it was supposed that the contribution of low-temperature Curie–Weiss paramagnetism characterizing the interaction between localized magnetic moments points to magnetic impurities in the Al–Cu–Fe icosahedral phase. However, weak Curie–Weiss paramagnetism was later shown to be an intrinsic property of the Al–Cu–Fe icosahedral phase with superior quasicrystallinity [17]. As perfection of the icosahedral phase structure decays, the diamagnetic contribution decreases [9, 14]. At once, the Curie–Weiss contribution rises owing to increased concentration of Fe ions with local magnetic moments [14]. Breaking of strong covalent interaction is believed to reduce the diamagnetic term [18] and can be the cause of the magnetic state of Fe in the Al–Cu–Fe icosahedral phase. A similar mechanism of appearance of large local magnetic moments on Fe atoms was established by using first-principles calculations for various structural defects in noncanonical approximants (β(CsCl)–Al–Cu–Fe solid solution and β-based ordered η-AlCu(Fe) phase) [19, 20]. Therefore, the study of the Curie–Weiss paramagnetic contribution is of interest for characterization of the interaction between the local magnetic moments induced by structural defects of the Al–Cu–Fe ι-phase and its approximants.

The Curie–Weiss term is known to have a negative Curie temperature for the Al–Cu–Fe icosahedral phase [14, 17], which is indicative of an antiferromagnetic interaction between localized magnetic moments. However, the type of the interaction between localized moments is still unclear for the Al–Cu–Fe approximants. It is even more intriguing to find out whether the Al–Cu–Fe approximants exhibit an antiferromagnetic interaction between the localized magnetic moments and how the characteristics of this interaction, the Curie temperature in particular, can be varied in the series of Al–Cu–Fe phases — noncanonical approximant, rational approximant, icosahedral quasicrystal, where the density of states at the Fermi level decreases.

In this work we study the parameters of the Curie–Weiss paramagnetic contribution, such as the Curie temperature and Curie constant, in the following se-

ries of Al–Cu–Fe phases: β(CsCl)-solid state solution, noncanonical approximant (η-AlCu(Fe) phase), rational approximants (P1+P2-pentagonal phases), icosahedral quasicrystal. For this series, in which the effects of the complex cluster local structure become more pronounced from β-solid state solution to icosahedral quasicrystal, we estimate the density of states at the Fermi level (N_F) using low-temperature heat capacity measurements and first-principles calculations. We show that the density of states at the Fermi level lowers and the absolute values of the negative Curie temperature fall consistently in these series of Al–Cu–Fe phases. We consider the observed correlations in terms of the antiferromagnetic Ruderman–Kittel–Kasuya–Yosida (RKKY) interaction between the local magnetic moments on Fe induced by intrinsic structural defects.

2. Experimental details

2.1. Preparation and structural characterization of Al–Cu–Fe alloys

The Al–Cu–Fe alloys were melted from components with purity not less than 99.9% in an arc furnace under very-high-purity helium atmosphere. For homogenization, the ingots were re-melted five times; each time upon melting the ingots were turned over. At all stages, the weight of the ingots was controlled. Then 50–100 mg of the as-prepared material were melted in suspended drop under helium atmosphere ($P_{He} \approx 10^{-3}$ mm Hg). The melt was quenched upon falling of the drop on a disc surface cooled with water. The alloys of the compositions $Al_{50}Cu_{33}Fe_{17}$, $Al_{50}Cu_{44}Fe_6$, $Al_{62}Cu_{25.7}Fe_{12.3}$ were prepared. Isothermal treatment was performed in He atmosphere to prepare the desired phase composition. Local chemical analysis was carried out by electron probe X-ray microanalysis using a JSM9600LV instrument. The local composition was analyzed on the basis of JSM9600LV references using Phi-Pho-Z software.

The structure of the annealed Al–Cu–Fe alloys was investigated by transmission electron microscopy using a JEM-200CX facility and by X-ray method. The obtained electron-diffraction patterns confirmed the formation of the following series of phases: β(CsCl)–$Al_{50}Cu_{33}Fe_{17}$, η-$Al_{50}Cu_{44}Fe_6$, P1+P2-$Al_{62}Cu_{25.7}Fe_{12.3}$, ι-$Al_{62}Cu_{25.7}Fe_{12.3}$. Typical electron-diffraction patterns are shown in Fig. 1.

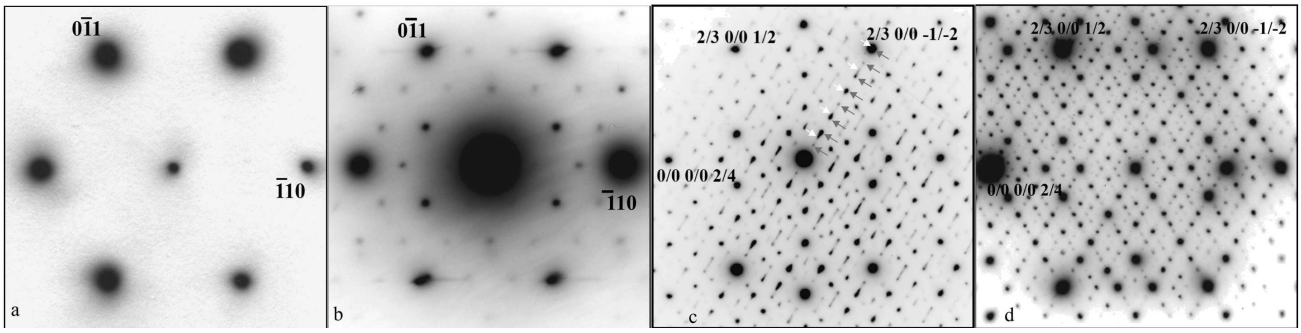

Fig. 1. Electron-diffraction patterns of the Al–Cu–Fe alloys with structure: (a) β-solid solution, [111] zone axis; (b) β-based ordered η-AlCu(Fe), domains with orientations type of $[301]_\eta$ and $[011]_\eta$; (c) P1+P2 pentagonal phases, (d) icosahedral phase, orientation along twofold symmetry axis [0/0 0/2 0/0]. The periodic reflections of P1 and P2 phases are shown by the white and grey arrows.

2.2. Measurements of physical properties

The magnetic susceptibility was measured in the temperature interval 2–400 K in a magnetic field of 50 kOe using a Quantum Design MPMS-XL5 magnetometer. The heat capacity measurements were performed by the relaxation method on a Quantum Design PPMS device in the temperature range 1.8–400 K.

2.3. Calculation technique and structural models

The electronic structure of the β(CsCl)–AlCu(Fe) solid solution and β-based ordered η-AlCu(Fe) phase was studied using the projector augmented waves (PAW) method as implemented in the Vienna *ab initio* simulation package (VASP) [21, 22] and the generalized gradient approximation (GGA) technique introduced by Perdew, Burke, and Ernzerhof (PBE) for the exchange-correlation potential [23]. We used a kinetic energy cut-off of 350 eV for the expansion of valence orbitals in plane waves and a $5\times5\times5$ Monkhorst–Pack k-point mesh, which were sufficient for total energy calculations with convergence better than 0.01 eV/atom. All the calculations were spin-polarized. The β-alloys of the composition $Al_{50}Cu_{31.3}Fe_{18.7}$ and $Al_{50}Cu_{43.8}Fe_{6.2}$ were simulated with a supercell containing eight unit cells (16 atoms) of the FeAl-phase with a CsCl-type structure (S.G. $Pm\bar{3}m$). The η-alloy of the composition $Al_{50}Cu_{45}Fe_5$ was simulated with one unit cell (20 atoms) of the low-temperature modification of η_2-AlCu phase (S.G. $I12/m1$) [24]. Copper and iron atoms were located in the same sublattice.

3. Results and discussion

Figure 2 shows the temperature function of magnetic susceptibilities χ for the Al–Cu–Fe alloys having the structures of β(CsCl)-solid solution, η-ordered phase (noncanonical approximant), P1+P2-pentagonal phases (canonical rational approximants) and icosahedral phase. The magnetic susceptibility function for the Al–Cu–Fe alloys is known to consist of three contributions: the low-temperature Curie–Weiss paramagnetic term (χ_{CW}), diamagnetic term (χ_{diam}) and temperature-dependent correction $\chi(T)$ including the Pauli paramagnetic term [8, 14, 17]. As expected, in the aforementioned phases the diamagnetic contribution increases from β(CsCl)--solid solution to icosahedral phase and the canonical approximant and icosahedral phase exhibit negative susceptibility in the whole investigated temperature interval. The Curie–Weiss paramagnetic contribution determined by the function

$$\chi_{\mathrm{CW}} = \chi_{0\mathrm{CW}} + C/(T-\Theta), \qquad (1)$$

where $\chi_{0\mathrm{CW}}$ is a temperature independent term, and C and Θ are the Curie constant and the Curie temperature, is fitted in the temperature range 10–40 K. The fitting range on the low-temperature side was limited to 10 K not to violate the relation $\mu H/k_{\mathrm{B}}T \ll 1$. The parameters of the Curie–Weiss paramagnetic contribution for the Al–Cu–Fe alloys obtained by the least-squares fitting are listed in Table.

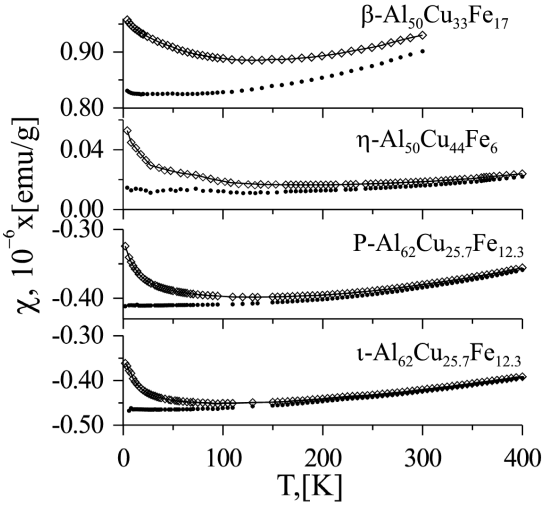

Fig. 2. Temperature function of magnetic susceptibilities χ for the Al–Cu–Fe alloys. The dotted lines show $\chi - \chi_{\mathrm{CW}}$ terms.

TABLE

Magnetic and electronic parameters of Al–Cu–Fe phases.

Phase	C_{CW} $[\frac{\mu\mathrm{emuK}}{g}]$	χ_0 $[\frac{\mu\mathrm{emu}}{g}]$	Θ [K]	γ $[\frac{mJ}{molK^2}]$
β-$Al_{50}Cu_{33}Fe_{17}$	6.21	0.86	−37.7	1.64
η-$Al_{50}Cu_{44}Fe_6$	0.816	0.013	−22.4	0.88
(P1+P2)-$Al_{62}Cu_{25.7}Fe_{12.3}$	1.313	−0.410	−13	0.48
ι-$Al_{62}Cu_{25.7}Fe_{12.3}$	1.162	−0.465	−7	0.29

In addition to the increase in the diamagnetic contribution (χ_{diam}), we find another essential correlation in the behavior of the Curie–Weiss paramagnetic parameters for the above series of Al–Cu–Fe phases. It can be seen (Table) that the Curie–Weiss terms of all the phases have negative values of the Curie temperature, and the absolute values of the Curie temperature fall consistently in this series from β-solid state solution to icosahedral phase. The reduction of the absolute values of negative Curie temperatures means that the antiferromagnetic interactions of local magnetic moments decrease in the series of Al–Cu–Fe phases [25]. For all the examined phases, the concentrations of local magnetic moments are about 10^{-3} as estimated from the Curie constant values. Here, the local magnetic moment on Fe is taken to be near to 2 μ_{B}. Direct exchange interaction can hardly be essential at such small concentrations of magnetic moments. Basing on these estimations, we can draw a conclusion about indirect exchange antiferromagnetic interaction of local magnetic moments in the considered Al–Cu–Fe phases.

Consistent decrease in RKKY-exchange in the series of Al–Cu–Fe phases can be due to several reasons: reduction in the concentration and magnitude of localized magnetic moments, as well as in the density of states at the Fermi level [25]. No correlations between the Curie temperature and Curie constants and therefore between the Curie temperature and the concentrations of localized magnetic moments are observed in the considered Al–Cu–Fe phases (Table). However, the density of states at the Fermi level is expected to fall in the series of Al–Cu–Fe phases, for which the complex cluster local structure features become more pronounced. Experiments have confirmed this tendency. Indeed, we find that the Sommerfield coefficient (γ) in the electronic component of heat capacity (γ), that is proportional to N_{F}, tends to decrease consistently in the following series of phases: β-solid solution, noncanonical η-approximant, P1 and P2 canonical approximants, icosahedral quasicrystal (Table).

A lower density of states at the Fermi level for the β-solid solution than for the ordered η-phase agrees completely with the data obtained by first-principles calculations. Figure 3 shows the calculated total and partial densities of 3d-Fe states for β-solid solutions of the compositions $Al_{50}Cu_{31.3}Fe_{18.7}$ and $Al_{50}Cu_{43.8}Fe_{6.2}$ and for the ordered η-$Al_{50}Cu_{45}Fe_5$ phase. It can be seen that the decrease in the density of states at the Fermi level in the series: β-solid solution $Al_{50}Cu_{33}Fe_{17}$ — η-$Al_{50}Cu_{44}Fe_6$ phase — is determined essentially by the reduction of the contribution from the 3d-Fe states.

Thus, we find a correlation between the values of the Curie temperature and the density of states at the Fermi level in the series of Al–Cu–Fe phases (β-solid state solution–approximants–icosahedral quasicrystal). Both parameters, the absolute values of negative Curie temperatures and N_{F}, lower in this series of alloys. In addition, the absolute values of negative Curie temperature decrease consistently (from −9.9 to −6.07 K) for a set of quasicrystalline AlCuFe12 alloys, for which the concentration of free carriers and consequently the density of

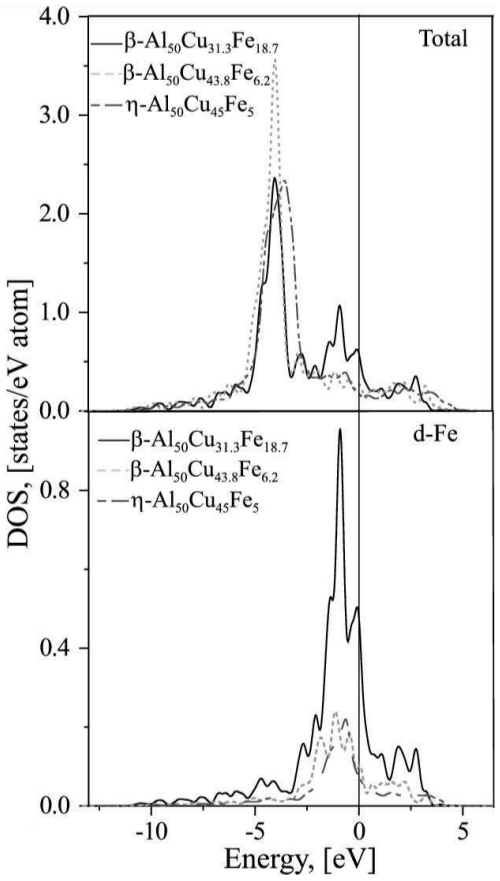

Fig. 3. Total density of states and partial density of the Fe $3d$ states for β(CsCl)–$Al_{50}Cu_{1-x}Fe_x$ solid solutions and ordered η-AlCu(Fe) phase.

states at the Fermi level (N_F) also lower [14]. Let us note that for the considered series of Al–Cu–Fe alloys having varying concentrations of local magnetic moments, we observe a near-linear relationship between the absolute Curie temperatures values and the estimated density of states at the Fermi level (see Table). The observed correlations are considered to be due to exchange antiferromagnetic interactions between localized magnetic moments in the Al–Cu–Fe alloys.

We believe that indirect exchange antiferromagnetism observed in the investigated Al–Cu–Fe phases determines the interaction between the localized magnetic moments induced by structural defects. Previously, first-principles calculations showed that the structural defects such as lattice vacancies and antisite defects Fe_{Al} lead to the appearance of localized magnetic moments in β(CsCl)–AlCu(Fe) solid solutions and in the ordered η-AlCu(Fe) phase [19, 20]. Antisite defects characterize the degree of order in β(CsCl)- and η-phases. For the ordered state of these phases, Fe atoms are localized in the $3d$-Me sublattice and have the maximum of Fe–Al bonds in the first coordination polyhedron. The Fe $3d$–Al s,p hybridization strongly diminishes the exchange coupling and results in the nonmagnetic state of Fe in β-AlCu(Fe) and η-AlCu(Fe), that agrees with the well-known effect of aluminum on the reducing of magnetism in ordered and disordered Fe–Al alloys [26–29]. For Fe_{Al3} localization, exchange coupling splits the spin-up and spin-down Fe $3d$ states. Electron rearrangement from the spin-down to spin-up Fe $3d$-states enhances the iron magnetic moment up to 2.7 μ_B. Besides, distortions of the coordination polyhedrons Al–Fe(Cu) and the increase in the interatomic Al–Fe distances can also lead to electron rearrangement from spin-down to spin-up Fe $3d$-states and to enhancement of magnetic moments on Fe [29].

We also assume that there are similar structural defects of the equilibrium and quenching types in the icosahedral Al–Cu–Fe phase, that is an ordered F-type quasicrystalline phase, and in its canonical approximants. The antisite defects and distortions of the icosahedral and dodecahedral coordination polyhedrons can result in Fe $3d$–Al $3p$ hybridization weakening, electron rearrangement from spin-down to spin-up Fe $3d$-states, and in the appearance of nonzero localized magnetic moments on Fe. The magnitudes of these magnetic moments can be estimated by first-principle calculations for the 1/1 canonical approximant of the Al–Cu–Fe icosahedral phase. There is an additional circumstantial argument in support of the occurrence of structural defects, which give rise to localized magnetic moments in the icosahedral Al–Cu–Fe phase. It is known that the degree of order of the Al–Cu–Fe icosahedral phase increases with structural perfection [30]. Consistent reduction of the Curie constant and therefore of the concentration of magnetic moments takes place in the series of Al–Cu–Fe icosahedral alloys, where the concentration of free carriers (N_F) also lowers consistently with improving structural perfection [14].

4. Conclusion

We found that the low-temperature Curie–Weiss paramagnetic contribution for the series of Al–Cu–Fe phases: β(CsCl)-solid state solution, noncanonical approximant (η-AlCu(Fe) phase), rational approximants (P1+P2--pentagonal phases), icosahedral quasicrystal — is characterized by negative Curie temperatures. A consistent decrease in the absolute values of the Curie temperature is revealed for this series.

For the examined Al–Cu–Fe phases, the decrease in the Curie temperature values correlates with the reduction of the density of states at the Fermi level estimated from low-temperature heat capacity measurements and first--principles calculations.

We consider the observed correlation to be related to the antiferromagnetic indirect exchange interaction (RKKY-interaction) between the localized magnetic moments on Fe ions in the Al–Cu–Fe phases. The main mechanism of the appearance of the localized magnetic moments is suggested to be weakening of covalent binding and Fe $3d$–Al s,p hybridization owing to intrinsic structural defects such as vacancies, antisite defects and distortions of coordination polyhedrons.

Acknowledgments

The study was supported by the Ural Department of RAS research program, project No. 12-U-2-1028.

References

[1] A.P. Tsai, A. Inoue, T. Masumoto, *Jpn. J. Appl. Phys.* **26**, 1505 (1987).

[2] N. Menguy, M. Audier, P. Guyot, M. Vacher, *Philos. Mag. B* **68**, 595 (1993).

[3] M. Quiquandon, A. Quivy, J. Devaud, F. Faudot, S. Lefebvre, M. Bessiere, Y. Calvayrac, *J. Phys., Cond. Matter* **8**, 2487 (1996).

[4] C. Dong, *Scr. Metall. Mater.* **33**, 239 (1995).

[5] C. Dong, Q.H. Zhang, D.H. Wang, Y.M. Wang, *Eur. Phys. J. B* **6**, 25 (1998).

[6] T. Klein, A. Gozlan, C. Berger, F. Cyrot-Lackmann, Y. Calvayrac, A. Quivy, *Europhys. Lett.* **13**, 129 (1990).

[7] T. Takeuchi, U. Mizutani, *J. Alloys Comp.* **342**, 416 (2002).

[8] S. Matsuo, H. Nakano, T. Ishimasa, Y. Fukano, *J. Phys., Cond. Matter* **1**, 6893 (1989).

[9] T. Klein, C. Berger, D. Mayou, F. Cyrot-Lackman, *Phys. Rev. Lett.* **66**, 2907 (1991).

[10] Z.M. Stadnik, D. Purdie, M. Garnier, Y. Bayer, A.P. Tsai, A. Inoue, K. Edagawa, S.T. Takeuchi, *Phys. Rev. Lett.* **77**, 1777 (1996).

[11] G.T. de Laissardiere, T. Fujiwara, *Phys. Rev. B* **50**, 5999 (1994).

[12] U. Mizutani, *J. Phys., Cond. Matter* **10**, 4609 (1998).

[13] K. Kirihara, T. Nagata, K. Kimura, K. Kato, M. Takata, E. Nishibori, M. Sakata, *Phys. Rev. B* **68**, 014205 (2003).

[14] N.I. Shchegolikhina, N.Yu. Kuz'min, A.F. Prekul, *Phys. Met. Metallogr.* **97**, 352 (2004).

[15] E.V. Shalaeva, M.V. Kuznetsov, A.F. Prekul, N.I. Shchegolikhina, *Bull. Russ. Acad. Sci., Phys.* **71**, 628 (2007).

[16] E.V. Shalaeva, A.F. Prekul, *Philos. Mag.* **91**, 589 (2011).

[17] J. Dolinsek, S. Vrtnik, M. Klanjsek, Z. Jaglicic, A. Smontara, I. Smiljanic, A. Bilusic, Y. Yokoyama, A. Inoue, C.V. Landauro, *Phys. Rev. B* **76**, 054201 (2007).

[18] A.F. Prekul, N. Kuz'min, N.I. Shchegolikhina, *Phys. Met. Metallogr.* **96**, 160 (2003).

[19] E.V. Shalaeva, N.I. Medvedeva, I.R. Shein, *Phys. Solid State* **49**, 1253 (2007).

[20] E.V. Shalaeva, N.I. Medvedeva, *Philos. Mag.* **92**, 1649 (2012).

[21] G. Kresse, J. Furthmuller, *Phys. Rev. B* **54**, 11169 (1996).

[22] G. Kresse, J. Hafner, *Phys. Rev. B* **47**, 558 (1993).

[23] J.P. Perdew, J.A. Chevary, S.H. Vosko, K.A. Jackson, M.R. Pederson, D.J. Singh, C. Fiolhais, *Phys. Rev. B* **46**, 6671 (1992).

[24] L.V. Rasin, N.S. Rudashevsky, L.N. Vyaltsov, *Zapiski Vsesoyuznogo Mineralogicheskogo Obshchestva* **114**, 90 (1982) (in Russian).

[25] S. Blundell, *Magnetism in Condensed Matter*, Oxford Univ. Press, New York 2001.

[26] J. Bogner, W. Steiner, M. Reissner, P. Mohn, P. Blaha, K. Schwarz, R. Krachler, H. Ipser, B. Sepiol, *Phys. Rev. B* **58**, 14922 (1998).

[27] N.I. Kulikov, A.V. Postnikov, G. Borstel, *Phys. Rev. B* **59**, 6824 (1999).

[28] G.P. Das, B.K. Rao, P. Jena, S.C. Devi, *Phys. Rev. B* **66**, 184203 (2002).

[29] E. Apinaniz, F. Plazaola, J.S. Gartaonandia, *Eur. Phys. J. B* **31**, 167 (2003).

[30] A.-P. Tsai, *Sci. Technol. Adv. Mater.* **9**, 013008 (2008).